How Do Mutations at Phenylalanine-153 and Isoleucine-155 Partially Suppress the Effects of the Aspartate-27 → Serine Mutation in *Escherichia coli* Dihydrofolate Reductase? †

Amanda Dion,‡ Charles E. Linn,‡ Thomas D. Bradrick,§ S. Georghiou,§ and Elizabeth E. Howell*,‡

Department of Biochemistry, University of Tennessee, Knoxville, Tennessee 37996-0840, and Molecular Biophysics Laboratory, Department of Physics, University of Tennessee, Knoxville, Tennessee 37996-1200

Received September 16, 1992; Revised Manuscript Received January 5, 1993

ABSTRACT: Several second-site suppressors of the D27S lesion in *Escherichia coli* dihydrofolate reductase (DHFR) have been identified. The activity of the primary mutant, D27S DHFR, was found to be greatly decreased at pH 7.0, consistent with aspartic acid-27 being critically involved in proton donation during catalysis. Partial suppressors of the D27S mutation have been selected by their ability to confer an increased resistance to trimethoprim upon host *E. coli*; the suppressors have been identified as F153S or I155N substitutions. D27S+F153S and D27S+I155N DHFRs display 2–3-fold increases in k_{cat} over D27S DHFR values, but only the F153S mutation decreases the K_m for dihydrofolate by a factor of 2. Neither double mutant approaches wild-type DHFR activity. Unexpectedly, Phe153 and Ile155 occur on the surface of the protein and are approximately 8 and 14 Å distant from the active site. Ile155 is a member of a β-bulge. A previously identified suppressing mutation, F137S, occurs nearby and is also a member of the same β-bulge [Howell et al. (1990) *Biochemistry 29*, 8561–8569]. Clustering of these three second-site mutations indicates this area of the structure may be important in protein function. Conformational changes due to the presence of these suppressing mutations are likely as the F153S and I155N mutations do not affect hydride-transfer rates upon introduction in wild-type DHFR and alterations in circular dichroism spectra are associated with the double-mutant DHFRs.

Dihydrofolate reductase (DHFR;[1] EC 1.5.1.3) catalyzes the NADPH-dependent reduction of dihydrofolate (DHF) to tetrahydrofolate (THF). THF cofactors are essential in biosynthetic reactions involving the transfer of one-carbon units and are required for the synthesis of thymidylate, purine nucleotides, and other metabolic intermediates. Several clinically important inhibitors of DHFR include the antitumor drug methotrexate (MTX), the antibacterial drug trimethoprim (TMP), and the antimalarial pyrimethamine.

A detailed reaction mechanism for this model enzyme has been proposed, and *Escherichia coli* DHFR designated a maximally evolved enzyme (Uchimaru et al., 1989; Fierke et al., 1987a,b). DHFR has also been studied extensively using NMR spectroscopy and X-ray crystallography techniques (Bolin et al., 1982; Filman et al., 1982; Bystroff et al., 1990; Bystroff & Kraut, 1991; Falzone et al., 1990, 1991). These structure analyses have delineated important interactions between ligands and the enzyme which have been probed by site-directed mutagenesis experiments in an effort to define the roles of specific amino acids in ligand binding and catalysis (Howell et al., 1986; Murphy & Benkovic, 1989; Adams et al., 1989, 1991; Warren et al., 1991).

A series of in vitro mutagenesis experiments have analyzed the mechanism of protonation in *E. coli* DHFR. For example, one mutant generated was Asp27 → Asn (D27N; Howell et al., 1986). Aspartic acid-27 is important in proton donation during catalysis, so it is not surprising the efficiency of the D27N mutant is decreased by a factor of 1.2×10^4 at pH 7.0. However, the D27N DHFR has an altered pH profile such that catalysis increases rapidly as pH decreases. These results indicate the enzyme-mediated protonation step can be bypassed if preprotonated substrate is bound by the mutant enzyme. A primary site revertant of the D27N DHFR gene was selected by the ability to confer an increased resistance to TMP upon host *E. coli*. This mutant, Asp27 → Ser (D27S), is 1500 times less active than wild-type (wt) DHFR, but is 3 times better than the D27N "parent" DHFR.

Using a pseudoevolutionary approach to understand the compensatory mechanisms available to protein structure in suppressing mutational effects, second-site suppressors of the D27S DHFR gene have been genetically selected. A second-site mutation previously identified in the D27S DHFR gene corresponds to Phe137 → Ser (F137S; Howell et al., 1990). This pseudorevertant displays a 2–3-fold decrease in K_m and a 3-fold increase in k_{cat}; therefore, the overall effect on k_{cat}/K_m is a 7–8-fold increase when compared to the D27S single mutant. In our present study, two additional suppressors of the D27S DHFR gene have been identified as Phe153 → Ser (F153S) and Ile155 → Asn (I155N).

The partial ability of these three mutations to suppress the effect of the D27S lesion is surprising as all three mutations cluster on the surface of DHFR, 8–15 Å distant from the active site. They would not have been predicted to affect catalytic efficiency from this position in the structure. F137 and I155 are members of a classic β-bulge. Since these three suppressing mutations occur at the carboxy terminus and the

† This research was supported by NIH Grants GM35308 (to E.E.H.) and GM38236 (to S.G.).

‡ Department of Biochemistry.

§ Department of Physics.

[1] Abbreviations: DHFR, dihydrofolate reductase; hDHFR, human dihydrofolate reductase; TMP, trimethoprim; MTX; methotrexate; DHF, dihydrofolate; THF, tetrahydrofolate; wt, wild type; $NADP^+(H)$, nicotinamide adenine dinucleotide phosphate (oxidized/reduced); CD, circular dichroism; SDS–PAGE, sodium dodecyl sulfate–polyacrylamide gel electrophoresis. Mutant enzymes containing amino acid substitutions are described by the wild-type residue and numbered position in the sequence, followed by the amino acid substitution. For example, D27S DHFR describes the Asp27 → Ser substitution in DHFR.

0006-2960/93/0432-3479$04.00/0

β-bulge is structurally conserved in bacterial DHFR, this region of the protein may be important in protein function.

MATERIALS AND METHODS

Isolation of Revertants. Two revertants of the mutant D27S DHFR gene carried in M13mp8 have been generated as previously described with minor modifications (Howell et al., 1990). In brief, mutagenesis was performed using a mutator strain of *E. coli*, DM2525 carrying the *mutD* allele (Wertman et al., 1984). This allele causes both transitions and transversions as well as deletions (Cox, 1976). DM2525 cells were infected with M13mp8 carrying the mutant D27S DHFR gene, and were grown overnight in rich media containing 200 μg of thymidine/mL. The latter turns on the mutator allele (Cox & Horner, 1983). Cells were then plated on M9 minimal media containing 100 μg of trimethoprim/mL (TMP). Trimethoprim is a potent, active-site-directed inhibitor of bacterial DHFR, and its presence in media allows selection of DHFR mutations (Burchall et al., 1982; Schimke, 1986; Then & Herman, 1981; Then, 1982). Since confluent growth of *E. coli* infected with M13–D27S DHFR (and also with M13–wt DHFR) occurs at ≤50 μg of TMP/mL, any colonies obtained after several days growth at higher TMP levels are putative revertants. As both wt and D27S DHFR genes confer resistance to similar TMP concentrations, primary-site revertants of D27S to wt DHFR are not selected.

Putative mutant viruses were removed from DM2525, and *E. coli* strain JM107 was infected to remove the virus from the *mutD* strain as well as to isolate mutations in the D27S DHFR–M13 phage from mutations in the host (e.g., membrane impermeability to TMP, mutations in the chromosomal DHFR gene, etc.; Dewes et al., 1986; Miller, 1972). Mutations affecting protein activity were assessed by Coomassie and activity stains of cell lysates run on nondenaturing gels. Other revertant types could involve mutations that weaken TMP binding or overproduce DHFR (Smith & Calvo, 1982; Flensburg & Skold, 1984; Haber et al., 1981; Grange et al., 1984). Increased DHFR production is readily assessed by Coomassie stains on native PAGE gels.

Mutations were identified by sequencing the entire gene. To increase protein expression, the mutant genes were cloned from M13mp8 into the high-copy plasmid pUC8. Mutant DHFRs were expressed in a *fol* strain of *E. coli* where the chromosomal DHFR gene has been deleted and replaced with a kanamycin resistance marker (Howell et al., 1988). This allows purification of mutant DHFRs that are not contaminated by wt DHFR due to expression of the *E. coli* chromosomal gene. Protein purification was performed as described previously (Howell et al., 1990).

Single-mutant DHFR genes were constructed from the double-mutant and wt DHFR genes by recombinant DNA techniques using *Eco*RI. The cutting pattern of this restriction enzyme allows separation of the D27S and F153S or I155N mutations. Single-mutant genes were verified by sequencing the entire gene.

Steady-State Kinetics. Steady-state data were obtained with a Perkin-Elmer λ3a spectrophotometer interfaced with an IBM PS2 according to Howell et al. (1987). The computer program UVSL3 (Softways, Moreno Valley, CA) was used to collect and analyze data. Assays were performed at 30 °C in a polybuffer containing 44 μM imidazole, 33 μM succinic acid, 44 μM diethanolamine, and 10 mM β-mercaptoethanol. This buffering system maintains a constant ionic strength between pH 4.5 and 9.5 (Ellis & Morrison, 1982). K_m values for DHF were obtained by maintaining NADPH at saturating concentrations (33–97 μM) and varying DHF at subsaturating concentrations (12–118 μM). Saturating NADPH concentrations were verified at each pH. Nonlinear regression (ENZFIT, Elsevier Science) was used to determine the k_{cat} and $K_{m(DHF)}$ values reported in the pH profiles below. K_m values for NADPH/NADPD were obtained by varying both DHF (13–115 μM) and cofactor (2.4–15.7 μM) concentrations at subsaturating levels; primary and secondary plots were calculated according to Cleland (1963). To eliminate any hysteretic behavior, DHFR was preincubated with either substrate or cofactor prior to initiation of the assay (Penner & Frieden, 1985). The pH–rate profiles were fit to

Scheme I

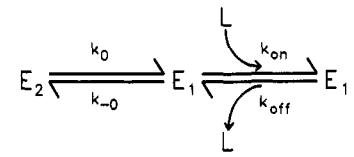

$$k = \log k_{max} - \log(1 + \chi^{pH-pK_a}) \quad (1)$$

where $k = k_{cat}$ or k_{cat}/K_m; k_{max} is the pH-independent value of k_{cat} or k_{cat}/K_m, and $\log \chi$ = slope (Murphy & Benkovic, 1989). This equation allows fitting of data displaying nonunity slopes.

NADPD, used to determine isotope effects, was prepared by reacting alcohol dehydrogenase from *Leuconostoc mesenteroides* (Boehringer Mannheim) with 1,1-dideuterioethanol (MSD Isotopes) and $NADP^+$ (Sigma). This reaction was coupled with $NADP^+$ aldehyde dehydrogenase to facilitate completion of the reaction (Howell et al., 1990). DHF was prepared by reduction of folic acid by sodium dithionite (Blakley, 1960) and stored at −70 °C in 5 mM HCl and 50 mM β-mercaptoethanol.

Rapid Kinetics. Pre-steady-state kinetic measurements were performed essentially as described previously (Fierke et al., 1987a; Dunn et al., 1990). Data were collected at 25 °C on a modified Aminco-Bowman DW-2 UV/vis spectrophotometer with an Analog Devices RTI 815 A/D converter for digitization of data (Bradrick & Georghiou, 1987; Sekharam et al., 1991). The dead time of this system is approximately 3 ms. In all of the experiments, the excitation wavelength was 290 nm, achieved using a 10-nm bandpass interference filter. The decrease in DHFR fluorescence accompanying NADPH binding was monitored using a Corning 7-39 filter. The final protein concentration was 0.4 μM. Fast and slow phases associated with the binding reactions were readily separated and recorded independently (0–180-ms vs 0–300-s time intervals). The fast rate was analyzed by a single-exponential decay followed by a linear rate:

$$F(t) = A \exp(-k_{obs}t) + k_a t + B \quad (2)$$

where $F(t)$ is the fluorescence intensity as a function of time, A is the amplitude of the quench, k_{obs} and k_a are the exponential and linear rates, respectively, and B is the final fluorescence. The linear rate corrects for the small contribution of the slow rate on the fast time scale. The slow rate was analyzed by a single-exponential decay only, and the first 2 data points (i.e., any contribution from the fast phase) out of a total of 1000 data points were excluded. A nonlinear fitting program (Marquardt algorithm) was employed to fit the data.

In 1981, Cayley et al. proposed a model describing the observed biphasic binding data. As depicted in Scheme I, two interconvertible conformations of DHFR exist (E_1 and E_2); however, NADPH binds to only one of these forms (E_1)

with high affinity. The fast phase in fluorescence quenching describes binding of NADPH to E_1 and the slow phase, the interconversion of E_2 to E_1.

Assuming that binding of NADPH to E_1 is a simple bimolecular reaction as shown in Scheme I, then the observed rate constant for the fast phase quench can be described by the equation:

$$k_{obs} = k_{on}[NADPH] + k_{off} \quad (3)$$

where k_{on} and k_{off} are association and dissociation rate constants, respectively.

In a second independent method used to determine k_{off}, fluorescence energy transfer was monitored in competition experiments (Dunn et al., 1978). Binding of NADPH to DHFR results in an increase in fluorescence at 450 nm due to energy transfer from the protein to NADPH. For the competition experiments, E·NADPH complex (1 μM enzyme preincubated for 20 min with 3 μM NADPH) was mixed with a large excess of $NADP^+$ (1 mM). When NADPH dissociates from E·NADPH, excess $NADP^+$ binds to free E, and the rate of decrease in energy transfer describes k_{off} for NADPH. This experiment assumes $k_{off(NADPH)} \ll k_{on(NADP^+)}[NADP^+] \gg k_{on(NADPH)}[NADPH]$. These conditions were confirmed by altering $NADP^+$ concentrations, which did not affect the observed rate. The decrease in fluorescence energy transfer was monitored using a Corning 3-71 filter.

For hydride-transfer measurements, a solution of enzyme and cofactor was mixed with dihydrofolate to give final concentrations of 15 μM DHFR, 120 μM DHF, and 125 μM NADPH. Fluorescence energy transfer was monitored, and traces were fit to eq 2. In this experiment, the initial exponential rate corresponds to the hydride-transfer rate while the linear rate describes the steady-state rate-determining step, which is release of the product, tetrahydrofolate (Fierke et al., 1987a).

All measurements were carried out at pH 7.0 in buffer containing 50 mM Tris, 25 mM Mes, 25 mM acetic acid, 10 mM β-merceptoethanol, and 100 mM NaCl.

Circular Dichroism. Circular dichroism spectra of 10 μM protein in 10 mM potassium phosphate, pH 7.0, buffer were obtained at 22 °C using a Jasco J720 spectropolarimeter. The cell path length was 2 mm. Ten spectra were acquired per sample using 1-nm steps and 2-s integrations, and an averaged spectrum was calculated. An essentially flat buffer base-line scan was then subtracted from the average protein scan to obtain the scans presented below. Spectral differences between mutant DHFRs are not due to dilution effects as spectra for each individual mutant are readily duplicated. The CD data are described as the mean residue ellipticity by taking 111 g/mol as the mean residue molecular mass.

Concentrations were determined using the following extinction coefficients: 28 000 M^{-1} cm^{-1} at 282 nm for DHF and folic acid (Blakley, 1960); 6220 M^{-1} cm^{-1} at 340 nm for NADPH (Horecker & Kornberg, 1948); 22 100 M^{-1} cm^{-1} at 302 nm, pH 13, or 23 250 M^{-1} cm^{-1} at 258 nm, pH 13, for MTX (Stone & Morrison, 1986); and 7250 M^{-1} cm^{-1} at 287 nm, pH 13, for TMP (Stone & Morrison, 1986). The molar extinction coefficient used to assess DHFR reduction of DHF was 12 300 M^{-1} cm^{-1} (Baccanari et al., 1975). Enzyme concentrations were determined by biuret assays, and all proteins were homogeneous according to SDS–PAGE. Enzyme inhibition titrations using the active-site inhibitor methotrexate were also performed to determine wt DHFR concentrations. The latter technique was not used to determine concentrations for mutant DHFRs containing the D27S mutation, since this mutation decreases enzyme affinity for MTX by a factor of 3000 (Howell et al., 1986).

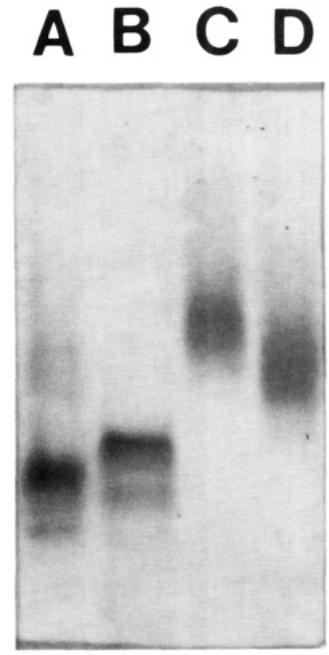

FIGURE 1: Altered mobilities of the mutant DHFRs compared to wt DHFR as determined by nondenaturing PAGE. The lanes contain the following proteins: (A) wt DHFR; (b) D27S DHFR; (C) D27S+I155N DHFR; (d) D27S+F153S DHFR. The bottom of the gel is the anode. Only one protein band is seen for these individual samples in SDS–PAGE. The faster migrating, minor bands in the wt and D27S DHFR (A and B) lanes are DHFRs, as determined by activity stains. Partial N-formylation or minor proteolysis could account for their altered mobilities. The bands for the double-mutant DHFRs are diffuse using both Coomassie and activity stains, suggesting a larger range of conformations may be available to the double-mutant DHFRs or a reduced stability or a greater tendency to aggregate under these conditions.

RESULTS

Isolation and Identification of Mutants. Two different revertants of the D27S DHFR gene carried in M13mp8 were isolated using increased resistance to TMP as a selection and relative activity in nondenaturing gels as a screening procedure. The revertant genes were sequenced, and one gene was found to possess a phenylalanine-153 (TTT codon) to serine (TCT) mutation, and the second revertant gene an isoleucine-155 (ATT) to asparagine (AAT) mutation. In both these genes, the D27S mutation was still present, and no other mutations were found.

The mobilities of the D27S+F153S and D27S+I155N mutant DHFRs in nondenaturing PAGE were found to be substantially altered as shown in Figure 1. Since neither of these mutations involves a change in charge, alteration of protein conformation must be associated with these mutations (Hames, 1990). We note that a previously identified suppressing mutation, F137S, only slightly decreases the mobility of D27S DHFR, even though the crystal structure of the D27S+F137S DHFR in complex with MTX suggests local conformation changes occur (Howell et al., 1990; K. Brown and J. Kraut, personal communication).

Steady-State Kinetics. The effects of the F153S and I155N mutations on D27S DHFR were initially evaluated using steady-state catalysis. The k_{cat}, $K_{m(DHF)}$, and $K_{m(NADPH)}$ values at pH 7.0 for wt, D27S, and the various mutant DHFRs are listed in Table I. The F153S or I155N suppressing mutations increase k_{cat} 2–4-fold over D27S values, but only the F153S

Table I: Steady-State Kinetic Values Determined at pH 7.0, 30 °C, for Various DHFRs

DHFR	k_{cat} (s^{-1})	$K_{m(DHF)}$ (μM)	$K_{m(NADPH)}$ (μM)	$K_{i(TMP)}$	^{D}V	$^{D}V/K$
wt	29 ± 1[a]	1.1 ± 0.2[a]	0.94 ± 0.36[a]	20 ± 8 pM[b]	1.2[c]	
D27S	0.41 ± 0.01[a]	56 ± 2[a]	1.3 ± 0.3[a]	2.9 ± 0.4 μM[a]	3.3[d]	3.1
D27S+F153S	1.56 ± 0.02	37 ± 2	1.1 ± 0.1	11 ± 3 μM	3.45 ± 0.04	3.09 ± 0.04
D27S+I155N	0.95 ± 0.02	55 ± 2	1.3 ± 0.3	5 ± 1 μM	3.3 ± 0.2	4.0 ± 0.3
F153S	22.8 ± 0.4	2.5 ± 0.3	nd[e]	nd	nd	nd
I155N	23.5 ± 0.4	4.3 ± 0.3	nd	nd	nd	nd

[a] From Howell et al. (1990). [b] From Stone and Morrison (1986). [c] pH 6.0; from Fierke et al. (1987a). [d] From Howell et al. (1987). [e] Not determined.

mutation decreases $K_{m(DHF)}$. The overall effects on the apparent second-order rate constant [$k_{cat}/K_{m(DHF)}$] in D27S DHFR by the F153S and I155N suppressing mutations are 6- and 2-fold increases, respectively. However, when compared to wt DHFR values, both double mutants display reduced activity. The D27S+F153S double mutant is 600-fold less efficient [$k_{cat}/K_{m(DHF)}$] and the D27S+I155N mutant is 1500-fold less efficient than wt DHFR. In comparison, D27S DHFR is 3600-fold less efficient than wt DHFR.

The pH profiles for k_{cat} and $k_{cat}/K_{m(DHF)}$ were determined for the double-mutant DHFRs and are shown in Figure 2. Both mutants continue to show the same effects described above throughout the pH range studied. At pH 5.0, the activities of the double-mutant DHFRs are near wt DHFR values, and the second-order rate constants [$k_{cat}/K_{m(DHF)}$] for D27S+F153S and D27S+I155N DHFRs are only 82- and 122-fold decreased with respect to wt values.

Since the F153S and I155N suppressing mutations were selected due to their ability to confer an increased resistance to TMP upon host *E. coli*, DHFR mutants that bind TMP less tightly could result. Therefore, we briefly assessed inhibition by TMP and obtained kinetic K_i values for the D27S+F153S and D27S+I155N DHFRs. Four different TMP concentrations (4–75 μM) were added to the assays. The DHF concentration was then varied in the presence of saturating NADPH concentrations. A replot of slope (obtained from Lineweaver–Burk plots) versus inhibitor concentration yielded K_i values of 11 ± 3 μM and 5.1 ± 1 μM for D27S+F153S and D27S+I155N DHFRs, respectively. For comparison, the TMP K_i's for wt and D27S DHFRs are 20 ± 8 pM and 2.9 ± 0.4 μM (Stone & Morrison, 1986; Howell et al., 1987). The presence of the F153S or I155N mutations in D27S DHFR weakens TMP binding by 4- and 2-fold, respectively. Apparently, the F153S and I155N mutations both increase catalytic efficiency and weaken TMP binding.

Isotope Effects. To evaluate whether these increases in steady-state k_{cat} values for D27S+F153S and D27S+I155N DHFRs have altered the rate-determining step in D27S DHFR catalysis, primary isotope effects were determined using NADPD. A substantial isotope effect [$^{D}V \sim 3$ where $^{D}V = k_{cat(NADPH)}/k_{cat(NADPD)}$] on hydride-transfer rates is observed from pH 5 to 9 for wt DHFR using stopped-flow techniques (Fierke et al., 1987a). However, when steady-state rates are monitored for wt DHFR, ^{D}V values of 3 are seen only at pH ≥9.0. These results support a change in the rate-determining step in wt DHFR, such that hydride transfer is only rate-determinig at high pH. In contrast, D27S DHFR shows a substantial isotope effect ($^{D}V \sim 3$) on steady-state rates from pH 5 to 9, indicating hydride-transfer rates have been decreased by the D27S mutation and hydride transfer is fully rate-determining.

NADPD isotope effects for D27S+F153S and D27S+I155N DHFRs are listed in Table I. These results show that even though the hydride-transfer rate is increased in these mutant enzymes, it is still rate-determining.

Does either the F153S or the I155N Mutation Affect Wt DHFR Kinetics? The ability of the F153S and I155N mutations to affect wt DHFR kinetics was evaluated by constructing genes coding for single mutants. We might expect effects on hydride-transfer rates as seen in the double-mutant DHFRs. However, to evaluate any effects on hydride-transfer rates in wt DHFR based mutants, steady-state kinetics at high pH values or stopped-flow kinetics need to be performed as the rate-determining step for wt DHFR catalysis at neutral pH is release of tetrahydrofolate. Above pH 8.4, hydride transfer becomes rate-determining.

Steady-state rates for wt, F153S, and I155N DHFRs at pH 7.0 are 29 ± 1, 22.8 ± 0.4, and 23.5 ± 0.4 s^{-1}, respectively, and $K_{m(DHF)}$ values are 1.1 ± 0.2, 2.5 ± 0.5, and 4.3 ± 0.3 μM, respectively. At pH 9.4, k_{cat} values are 3.0 ± 0.1, 2.65 ± 0.04, and 2.68 ± 0.06 s^{-1}, respectively, and $K_{m(DHF)}$ values are 1.4 ± 0.1, 2.2 ± 0.1, and 2.0 ± 0.1 μM, respectively.

Pre-steady-state hydride-transfer rates at pH 7.0 for wt, F153S, and I155N DHFRs are 238 ± 9, 242 ± 9, and 256 ± 9 s^{-1}, repectively. Addition of NADPD, instead of NADPH, routinely slowed down the hydride-transfer rates for all enzymes by a factor of approximately 3. Neither the F153S nor the I155N mutations have increased hydride-transfer rates; therefore, neither mutation is additive in the wt DHFR context.

Stopped-Flow Kinetic Analysis. The transient binding of ligands to DHFR has been previously studied by following the time-dependent quenching of intrinsic enzyme fluorescence upon complex formation or by the enhancement of NADPH fluorescence resulting from energy transfer upon complex formation (Dunn et al., 1978; Dunn & King, 1980; Cayley et al., 1981). Binary complex formation with NADPH for the *E. coli* enzyme is characterized by biphasic binding kinetics as shown in Figure 3A,B, where the fast-phase quench is a ligand concentration-dependent phase followed by a slow ligand-independent process. Biphasic kinetic traces have been interpreted by Cayley et al. (1981) as describing two interconvertible forms of the apoenzyme, E_1 and E_2, and only E_1 binds NADPH tightly. This model is depicted in Scheme I.

Apparent rate constants for the fast phase of NADPH binding to wt and four mutant DHFRs increase linearly with NADPH concentration as shown for three representative enzymes in Figure 3C. For a plot of k_{obs} versus [NADPH], the slope is k_{on} and the intercept is k_{off}. The rate constants determined by this method at pH 7.0 are given in Table II. The values are in good agreement with previously published numbers determined for wt, D27S, F137S, and D27S+F137S DHFRs (Fierke et al., 1987a; Appleman et al., 1990; Dunn et al., 1990). There were not any significant changes in k_{on} for any of the mutant DHFRs studied.

Recently Adams et al. (1989) have reported improved fitting of the fast phase of NADPH binding to wt DHFR using an equation that described two exponential processes. One exponential component described binding of NADPH to E_1; the second, binding of NADPH to E_2. The latter interaction

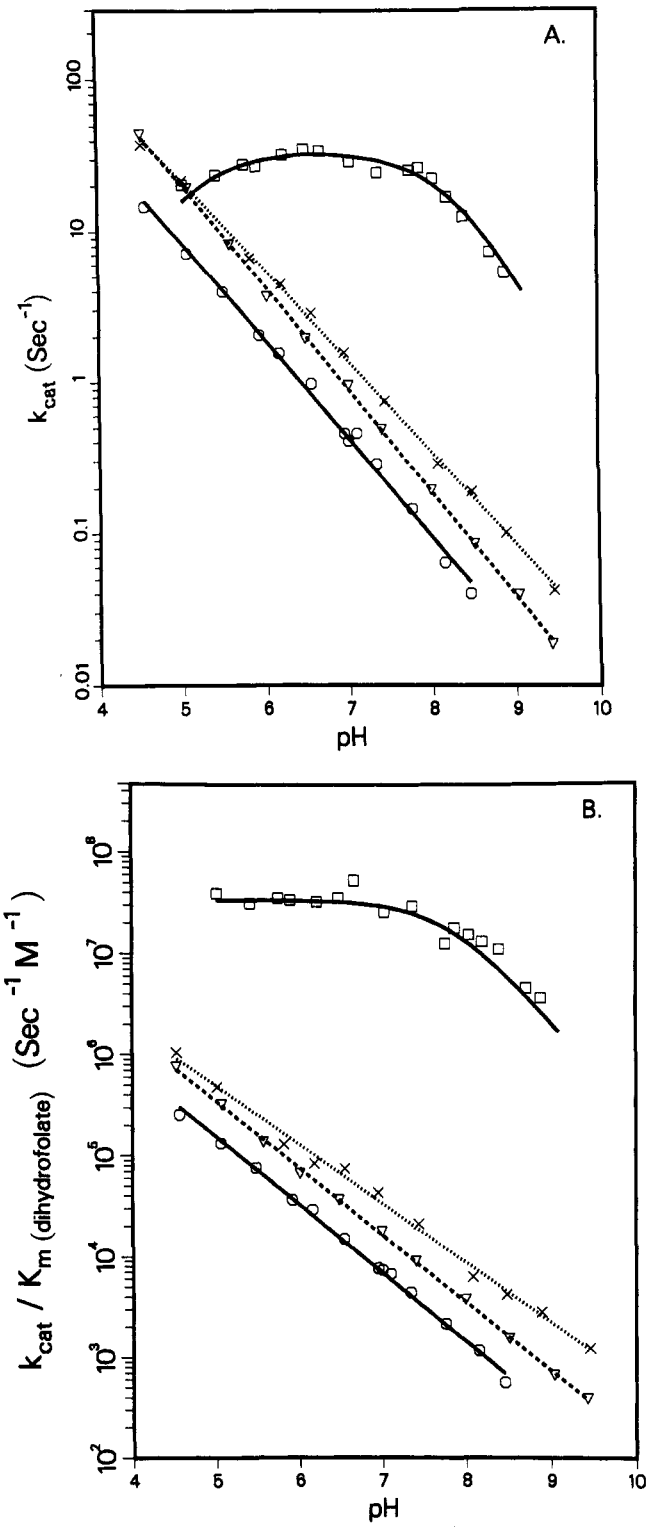

FIGURE 2: pH profiles of (A) k_{cat} and (B) $k_{cat}/K_{m(DHF)}$ for wild-type DHFR (□), D27S DHFR (○), D27S+F153S DHFR (×), and D27S+I155N DHFR (▽). Best-fit values to eq 1 are listed under Discussion.

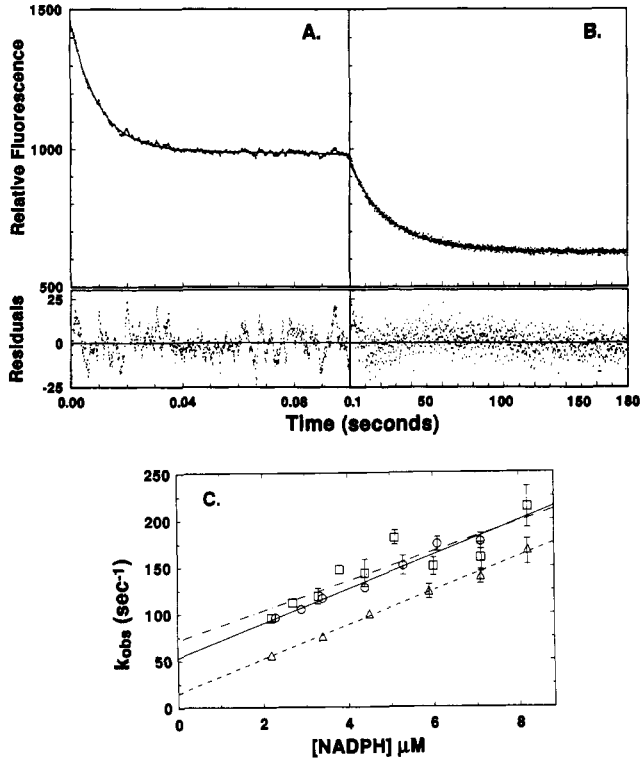

FIGURE 3: Representative stopped-flow kinetic traces of fast (A) and slow (B) phases of NADPH binding to the wild-type enzyme, showing the quenching of intrinsic protein fluorescence at pH 7.0. The traces were recorded independently at two different time scales, and data were fit as described under Materials and Methods. Residuals for the fits are additionally shown. The final DHFR and NADPH concentrations were 0.4 and 4 μM, respectively. Panel C shows the concentration dependence of the observed rate constant, k_{obs}, for the fast phase of NADPH binding to wt DHFR (△), D27S DHFR (□), and D27S+F153S DHFR (○). The data were fit to eq 3 as described in the text. Calculated rate constants are listed in Table II.

had an approximately 100-fold decreased affinity with respect to binding of NADPH to E_1. We do not observe a better fit of our fast-phase data to a two-exponential equation (Bevington, 1969).

k_{off} values determined by the above method are subject to large experimental errors (Appleman et al., 1990). To determine k_{off} values more accurately, competition experiments were employed (Dunn et al., 1978) where a preequilibrated enzyme·NADPH complex is mixed with a large excess of a competing ligand, $NADP^+$, and the decrease in fluorescence energy transfer is measured. This method requires a difference in fluorescence energy transfer between E·NADPH and E·$NADP^+$ complexes. The results from these experiments are listed in Table II. The most significant effects are seen with F153S and D27S+F153S mutant DHFRs where 2.5- and 1.8-fold increases for release of NADPH are observed over wt and D27S DHFR values.

Previously, Dunn et al. (1990) have interpreted large differences between k_{off} determined by relaxation and competition methods to support an alternate scheme where isomerization of E_1·NADPH to a second complex, E_1*·NADPH, occurs. We cannot exclude this possibility since our k_{off} values determined by these two methods differ by up to 20-fold.

Rates for the conversion of E_2 to E_1 calculated from the slow phase are 0.039 ± 0.002, 0.023 ± 0.002, 0.044 ± 0.002, 0.023 ± 0.002, 0.027 ± 0.003, and 0.055 ± 0.004 s^{-1} for wt, D27S, D27S+F153S, D27S+I155N, I155N, and F153S DHFRs, respectively.

In the absence of bound ligand, the equilibrium between conformers can be determined from a ratio of amplitudes for the slow and fast phases (=K_0; see Table II). The equilibrium shifts by approximately 2-fold for the five mutant DHFRs so that less of the enzyme population exists in the E_1 form at pH 7.0. The D27S, F153S, or I155N single mutations all affect this ratio when added to the wt DHFR context. Since the D27S, F153S, and I155N mutations affect K_0 to the same degree, the effects on K_0 are not additive in the double mutants.

Table II: Rate Constants for NADPH Binding in Wt, D27S, D27S+F153S, D27S+I155N, F153S, and I155N DHFRs According to Scheme I (pH 7.0, 25 °C)

rate constant	wt	D27S	D27S+F153S	D27S+I155N	F153S	I155N
k_{on} (μM^{-1} s^{-1})	18 ± 0.06	16 ± 3	18 ± 1	14 ± 2	22 ± 2	21 ± 2
k_{off}^{a} (s^{-1})	14 ± 3	69 ± 15	54 ± 6	93 ± 10	16 ± 11	71 ± 7
k_{off}^{b} (s^{-1})	4.2 ± 0.07	3.5 ± 0.1	6.5 ± 0.1	4.6 ± 0.1	10 ± 0.3	5.0 ± 0.2
$K_0 = k_{-0}/k_0^{c}$	0.80 ± 0.03	1.6 ± 0.2	1.4 ± 0.1	1.8 ± 0.1	1.5 ± 0.1	1.9 ± 0.2

[a] Determined from fast-phase relaxation experiments. [b] Determined from competition experiments. [c] Estimated from fluorescence amplitudes; K_0 = (amplitude of quench for slow phase)/(amplitude of quench for fast phase).

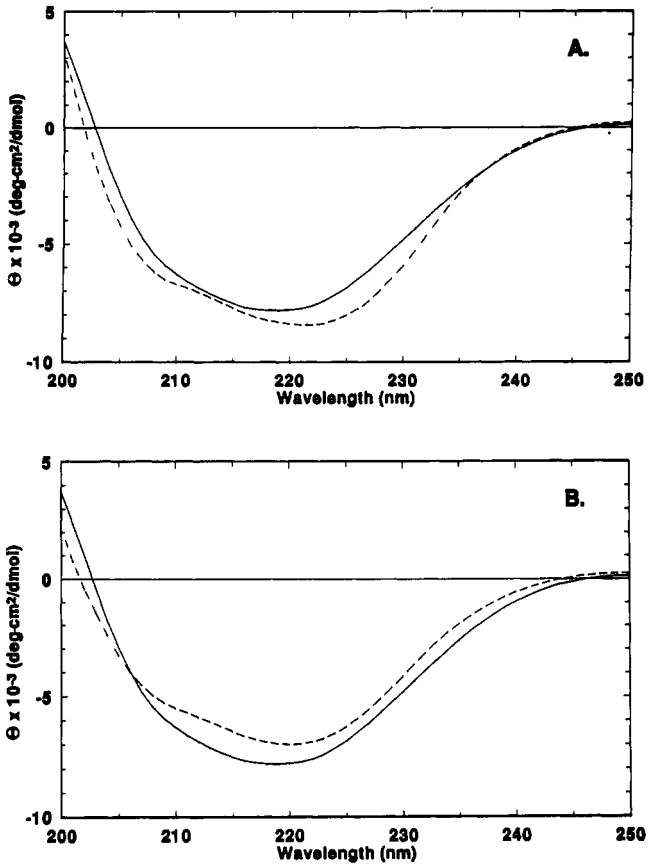

FIGURE 4: Circular dichroism spectra for wt (—) and double-mutant (- - -) DHFRs. (A) D27S+F153S DHFR; (B) D27S+I155N DHFR. θ is the molar ellipticity expressed in degrees cm^2 per decimole. An average spectrum calculated from 10 scans (minus a buffer base line) is shown for each protein. Spectra were readily reproduced.

Circular Dichroism Spectra. To assess the effects of the F153S and I155N mutations on D27S DHFR structure, circular dichroism spectra were obtained and are shown in Figure 4. The spectrum for wt DHFR (average of 10 scans) compares well with that determined by Kuwajima et al. (1991). The D27S DHFR spectrum differs only slightly from wt DHFR spectra (data not shown). However, both D27S+F153S and D27S+I155N double-mutant DHFRs consistently exhibit altered CD spectra. The spectral changes are not just intensity changes, since spectral shape changes are also observed. These results are compatible with structural perturbations.

DISCUSSION

Location of F153 and I155 Residues in E. coli DHFR. The partial ability of the F153S and I155N mutations to suppress the effect of the D27S lesion is surprising since the α-carbons of these amino acids are 8.2 and 13.6 Å distant from the α-carbon of D27S. As shown in Figure 5A, residues 153 and 155 occur on the surface of *E. coli* DHFR in β-strand H near the C-terminus (residue 158). I155 (along with V136, F137) is a member of an unusual structural element, a classic β-bulge. This local environment is depicted in Figure 5B. A β-bulge occurs when an additional amino acid is inserted into a β-strand and disrupts the normal hydrogen-bonding pattern (Richardson et al., 1978).

The role of β-bulges is not known. They may facilitate insertion or deletion of amino acids in β-strands rather than forcing changes in register (Richardson et al., 1978; Sondek & Shortle, 1990, 1992). Alternatively, β-bulges may be a way to twist strands in a right-handed direction which may have functional consequences (Matthews et al., 1989).

We have previously isolated a F137S mutation and identified it as a partial suppressor of D27S DHFR (Howell et al., 1990). F137 is a member of the same β-bulge as I155. This β-bulge is conserved in *Lactobacillus casei* DHFR although the amino acids involved are not the same. In chicken and human DHFRs, a β-blowout (six amino acids inserted) is observed. The observed clustering of three second-site mutations strongly suggests this area of the structure is more important than previously recognized.

All three suppressing mutations (F137S, F153S, F155N) flank W30, a member of α-helix B (residues 25–35). In wt DHFR, F153 and I155 stack directly with W30, and F137 interacts in an edge-on manner (Burley & Petsko, 1985). Since all three mutations substitute a hydrophilic amino acid for a hydrophobic one, changes in stacking behavior could alter the position of W30 and permute the conformation of the active site by moving α-helix B.

In fact, an X-ray structure of D27S+F137S DHFR in complex with methotrexate indicates the F137S mutation affects the active site (K. Brown and J. Kraut, personal communication). Specifically, the β-bulge is still present; however, residues 26, 27, 28, and 30 move approximately 0.3 Å. When the edge-on interaction between F137 and W30 is lost due to the F137S mutation, the indole ring of W30 flips approximately 180° into the active site. When W30 moves, it moves other members of the B α-helix. Another effect due to flipping of the indole ring is loss of a "conserved" water molecule (405). If these structural changes also occur when DHF is bound, altered contacts could explain the observed 2-fold decrease in $K_{m(DHF)}$ and concomitant 3-fold increase in k_{cat} for D27S+F137S DHFR. Whether the D27S+F153S and D27S+I155N mutant DHFRs also affect the position of W30 is not clear, however. More substantial changes might be expected since the mobilities of D27S+F153S and D27S+I155N DHFRs on nondenaturing PAGE gels are considerably altered, as are the CD spectra.

In human DHFR (hDHFR), Ratnam et al. (1988) have investigated the role of the homologous β-blowout (residues 164–169) using monoclonal antibodies against residues 140–186. Addition of this antibody to hDHFR surprisingly decreases activity, and, conversely, prior binding of ligands to hDHFR reduces antibody binding. More recently, Bullerjahn

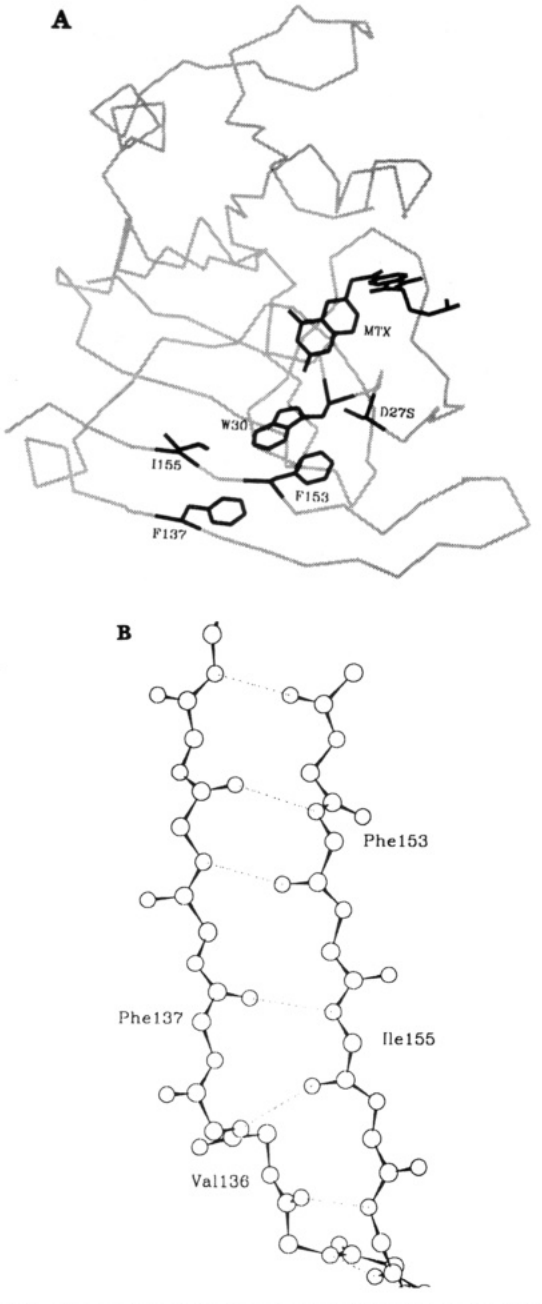

FIGURE 5: (A) α-Carbon backbone for the binary complex of *E. coli* D27S DHFR with methotrexate. Methotrexate and the side chains of S27, W30, F137, F153, and I155 are traced in heavy black. Approximate values for the shortest distances between these hydrophobic residues are the following: W30 to F137, 4.2 Å; W30 to F153, 3.5 Å; W30 to I155, 4.4 Å; F137 to F153, 5.2 Å; and F137 to I155, 4.1 Å. (B) Peptide backbone describing the local environment of a classic β-bulge composed of V136, F137, and I155. Hydrogen bonds are denoted by dashed lines; side chains are not shown for clarity. The alternating narrow, wide pairs of hydrogen bonds associated with antiparallel β-strands are seen at the top of the picture. The insertion of F137 into β-strand G causes the β-strand twist at the bottom of the picture.

and Freisheim (1992) have deleted two, four, and six amino acids from the β-blowout. Deletion of six amino acids abolishes enzyme activity and destabilizes hDHFR. Deletion of two or four amino acids decreases enzyme activity by approximately 33 or 38% and concurrently increases both K_m's approximately 10-fold. Freisheim and co-workers concluded the deletion mutants were less flexible and that conformational changes occurred at the β-blowout during ligand binding and catalysis.

Steady-State Kinetics. pH profiles for the double-mutant DHFRs as well as D27S DHFR differ drastically from wt DHFR profiles. Simple mechanisms describing both types of pH profiles have been previously described (Howell et al., 1987, 1990; Bystroff et al., 1990; Stone & Morrison, 1984). To summarize, the Asp27 residue in wt DHFR indirectly donates a proton through an intermediate water molecule to N5 of bound unprotonated DHF. This mechanism can be described by $HE + S \rightleftarrows HES \rightarrow$ products. In contrast, D27S-based DHFRs must utilize a proton from solution since they lack a proton donor. Therefore, protonated DHF [pK_a(N5) = 2.59; Maharaj et al., 1990] is the substrate for D27S-based DHFRs, and this situation can be described by $E + HS \rightleftarrows EHS \rightarrow$ products. Increased activity at low pH corresponds to increasing concentrations of protonated DHF as the pK_a of N5 is approached.

Steady-state kinetics data show the F153S and I155N suppressing mutations increase k_{cat} when added to the D27S DHFR context; however, only the F153S mutation decreases K_m for dihydrofolate. Fitting of the pH profile (Figure 2) to eq 1 yielded best-fit values for D27S, D27S+F153S and D27S+I155N DHFRs of $k_{cat,max} = 330 \pm 42$, 656 ± 41, and $937 \pm 54\ s^{-1}$, respectively, with $\chi = 4.5 \pm 0.1$, 4.0 ± 0.05, and 4.8 ± 0.06, respectively. A χ of 10 corresponds to a slope of 1. The differences in the pH-independent values for $k_{cat,max}$ indicate 2- and 3-fold increases in hydride-transfer rates for D27S+F153S and D27S+I155N DHFRs. Hydride transfer is still rate-determining in these enzymes as NADPD isotope effects yield ^DV values of approximately 3.

The F153S and I155N mutations do not affect hydride-transfer rates in the wt DHFR context as measured by both stopped-flow technqiues at pH 7.0 and steady-state rates at pH 9.4.

Ligand Binding. Rates for binding and release of NADPH from the wt and mutant DHFRs have been determined and compiled in Table II. No significant changes in k_{on} are observed. When k_{off} values from competition experiments are compared, both the F153S and D27S+F153S mutant DHFRs display an approximately 2-fold increase in off rates when compared to wt and D27S DHFRs. Since the F153S mutation is distant from the NADPH binding site, there must be long-range effects associated with this mutation.

Another indication of long-range effects can be seen by shifts in the equilibrium between the E_1 and E_2 conformers of the apoenzyme (K_0 in Table II). All three single-mutant DHFRs (D27S, F153S, I155N) show altered ratios, indicating numerous mutations at various points in the DHFR structure can affect this equilibrium.

Are Conformational Changes Associated with the F153S and I155N Mutations? Numerous observations support the notion of conformational changes occurring in D27S+F153S and D27S+I155N DHFRs. First, the nonadditivity of the F153S and I155N mutations to the wt and D27S DHFR contexts as measured by steady-state and stopped-flow kinetic techniques indicates conformational changes (Wells, 1990; Carter et al., 1984). Second, effects on release of NADPH in both the F153S and D27S+F153S DHFRs imply long-range effects perturbing the NADPH binding site. Third, migration in native PAGE gels monitors changes in protein charge and conformation. Both double mutants migrate much more slowly than either wt, D27S, or D27S+F137S DHFRs (Figure 1). Finally, changes in circular dichroism spectra indicate changes in protein conformation are associated with the D27S+F153S and D27S+I155N DHFR structures.

Changes in the position of W30 as seen for the D27S+F137S DHFR (K. Brown and J. Kraut, personal communication) could be associated with the F153S and I155N mutations as

these residues also flank W30. However, other changes in these double mutants might be expected since larger changes in CD spectra and also larger changes in mobility on native PAGE are observed.

Any detailed analysis of structural changes must await crystallization of these mutant enzymes. However, it is interesting to speculate that altered CD intensity could correspond to decreased β-strand twist, altered contributions of aromatic side chains, and/or changes in amino acid register that might accompany loss of a β-bulge (Applequist, 1982; Brahms & Brahms, 1980; Woody, 1985; Sondek & Shortle, 1990, 1992). An engineered deletion of F137 in the D27S DHFR gene has been constructed (unpublished results) to delete the β-bulge. A CD spectrum of the D27S+Δ137 DHFR is similar to the spectra for D27S+F153S and D27S+I155N DHFRs, suggesting loss of the β-bulge structure in all three mutant enzymes. Also supporting this hypothesis, the observed electrophoretic mobility of D27S+ΔF137 DHFR is similar to the mobilities of D27S+F135S and D27S+I155N DHFRs.

Conclusion. Second-site suppressors have been generated in other mutant enzymes, for example, ricin, T4 lysozyme, triosephosphate isomerase, and tryptophan synthetase (Kim et al., 1992; Poteete et al., 1991; Blacklow et al., 1991; Nagata et al., 1989). Since the suppressing mutations in these enzymes all occur in or near the catalytic site, minor restructuring of the catalytic site has been proposed as the mechanism for restoring partial activity. In contrast to these studies, our partial suppressors of D27S DHFR, 8–16 Å distant from the catalytic site, underscore the potential importance of residues outside the "traditional active site" in enzyme function.

ACKNOWLEDGMENT

We thank Joe Beechem, Vanderbilt University, for the use of his CD instrument.

REFERENCES

Adams, J. A., Johnson, K., Matthews, R., & Benkovic, S. J. (1989) *Biochemistry 28*, 6611–6618.

Adams, J. A., Fierke, C. A., & Benkovic, S. J. (1989) *Biochemistry 30*, 11046–11054.

Appleman, J. R., Howell, E. E., Kraut, J., & Blakley, R. L. (1990) *J. Biol. Chem. 265*, 5579–5584.

Applequist, J. (1982) *Biopolymers 21*, 779–795.

Baccanari, D., Phillips, A., Smith, S., Sinski, D., & Burchall, J. (1975) *Biochemistry 14*, 5267–5273.

Bevington, P. R. (1969) *Data Reduction and Error Analysis for the Physical Sciences*, p 200, McGraw-Hill, New York.

Blacklow, S. C., Liu, K. D., & Knowles, J. R. (1991) *Biochemistry 30*, 8470–8476.

Blakley, R. L. (1960) *Nature 40*, 1684–1685.

Bolin, J. T., Filman, D. J., Matthews, D. A., Hamlin, R. C., & Kraut, J. (1982) *J. Biol. Chem. 257*, 13650–13662.

Bradrick, T. D., & Georghiou, S. (1987) *Biochim. Biophys. Acta 905*, 494–498.

Brahms, S., & Brahms, J. (1980) *J. Mol. Biol. 138*, 149–178.

Bullerjahn, A. M. E., & Freisheim, J. H. (1992) *J. Biol. Chem. 267*, 864–870.

Burchall, J. J., Elwell, L. P., & Fling, M. E. (1982) *Rev. Infect. Dis. 4*, 246–254.

Burley, S. K., & Petsko, G. A. (1985) *Science 229*, 23–28.

Bystroff, C., & Kraut, J. (1991) *Biochemistry 30*, 2227–2239.

Bystroff, C., Oatley, S. J., & Kraut, J. (1991) *Biochemistry 29*, 3263–3277.

Carter, P. J., Winter, G., Wilkinson, A. J., & Fersht, A. R. (1984) *Cell 38*, 835–840.

Cayley, P. J., Dunn, S. M. J., & King, R. W. (1981) *Biochemistry 20*, 874–879.

Cleland, W. W. (1963) *Biochim. Biophys. Acta 67*, 104–137.

Cox, E. C. (1976) *Annu. Rev. Genet. 10*, 135–156.

Cox, E. C., & Horner, D. L. (1983) *Proc. Natl. Acad. Sci. U.S.A. 80*, 2295–2299.

Dewes, H., Ostergaard, H. L., & Simpson, L. (1986) *Mol. Biochem. Parasitol. 19*, 149–161.

Dunn, S. M. J., & King, R. W. (1980) *Biochemistry 19*, 766–773.

Dunn, S. M. J., Batchelor, J. G., & King, R. W. (1980) *Biochemistry 17*, 2356–2364.

Dunn, S. M. J., Lanigan, T. M., & Howell, E. E (1990) *Biochemistry 29*, 8569–8576.

Ellis, K. J., & Morrison, J. F. (1982) *Methods Enzymol. 87*, 405–426.

Falzone, C. J., Benkovic, S. J., & Wright, P. E. (1990) *Biochemistry 29*, 9667–9677.

Falzone, C. J., Wright, P. E., & Benkovic, S. J. (1991) *Biochemistry 30*, 2184–2191.

Fierke, C. A., Johnson, K. A., & Benkovic, S. J. (1987a) *Biochemistry 26*, 4085–4092.

Fierke, C. A., Johnson, K. A., & Benkovic, S. J. (1987b) *Cold Spring Harbor Symp. Quant. Biol. 52*, 631–638.

Filman, D. J., Bolin, J. T., Matthews, D. A., & Kraut, J. (1982) *J. Biol. Chem. 257*, 13663–13672.

Flensburg, J., & Skold, O. (1984) *J. Bacteriol. 159*, 184–190.

Grange, T., Kunst, F., Thillet, J., Ribadeau-Dumas, B., Mousseron, S., Hung, A., Jami, J., & Pictet, R. (1984) *Nucleic Acids Res. 12*, 3585–3601.

Haber, D. A., Beverly, S. M., Kiely, M. L., & Schimke, R. T. (1981) *J. Biol. Chem. 256*, 9501–9510.

Hames, B. D. (1990) *Gel Electrophoresis of Proteins: A Practical Approach* (Hames, B. D., & Rickwood, D., Eds.) Chapter 1, IRL Press, Oxford.

Horecker, B. L., & Kornberg, A. (1948) *J. Biol. Chem. 175*, 385–390.

Howell, E. E., Villafranca, J. E., Warren, M. S., Oatley, S. J., & Kraut, J. (1986) *Science 231*, 1123–1128.

Howell, E. E., Warren, M. S., Booth, C. L. J., Villafranca, J. E., & Kraut, J. (1987) *Biochemistry 26*, 8591–8598.

Howell, E. E., Foster, P. G., & Foster, L. M. (1988) *J. Bacteriol. 170*, 3040–3045.

Howell, E. E., Booth, C., Farnum, M., Kraut, J., & Warren, M. S. (1990) *Biochemistry 29*, 8561–8569.

Kim, Y., Mlsna, D., Monzingo, A. F., Ready, M. P., Frankel, A., & Robertus, J. D. (1992) *Biochemistry 31*, 3294–3296.

Kuwajima, K., Garvey, E. P., Finn, B. E., Matthews, C. R., & Sugai, S. (1991) *Biochemistry 30*, 7693–7703.

Maharaj, G., Selinsky, B. S., Appleman, J. R., Perlman, M., London, R. E., & Blakley, R. L. (1990) *Biochemistry 29*, 4554–4560.

Matthews, D. A., Appelt, K., & Oatley, S. J. (1989) *J. Mol. Biol. 205*, 449–454.

Miller, J. (1972) *Experiments in Molecular Genetics*, p 218, Cold Spring Harbor Laboratory, Cold Spring Harbor, NY.

Murphy, D. J., & Benkovic, S. J. (1989) *Biochemisty 28*, 3025–3031.

Nagata, S., Hyde, C. C., & Miles, E. W. (1989) *J. Biol. Chem. 264*, 6288–6296.

Penner, M., & Frieden, C. (1985) *J. Biol. Chem. 260*, 5366–5369.

Poteete, A. R., Dao-Pin, S., Nicholson, H., & Matthews, B. W. (1991) *Biochemistry 30*, 1425–1432.

Ratnam, M., Tan, S., Prendergast, N. J., Smith, P. L., & Freisheim, J. H. (1988) *Biochemistry 27*, 4800–4804.

Richardson, J. S., Getzoff, E. D., & Richardson, D. C. (1978) *Proc. Natl. Acad. Sci. U.S.A. 75*, 2574–2578.

Schimke, R. T. (1986) *Cancer 10*, 1912–1917.

Sekharam, K. M., Bradrick, T. D., & Georghiou, S. (1991) *Biochim. Biophys. Acta 1063*, 171–174.
Smith, D. R., & Calvo, J. M. (1982) *Mol. Gen. Genet. 187*, 72–78.
Sondek, J., & Shortle, D. (1990) *Proteins: Struct., Funct., Genet. 7*, 299–305.
Sondek, J., & Shortle, D. (1992) *Proteins: Struct., Funct., Genet. 13*, 132–140.
Stone, S. R., & Morrison, J. F. (1984) *Biochemistry 23*, 2753–2758.
Stone, S. R., & Morrison, J. F. (1986) *Biochim. Biophys. Acta 869*, 275–285.
Then, R. L. (1982) *Rev. Infect. Dis. 4*, 261–269.
Then, R. L., & Hermann, F. (1981) *Chemotherapy 27*, 192–199.
Uchimaru, T., Tsuzuki, S., Tanabe, K., Benkovic, S. J., Furukawa, K., & Taira, K. (1989) *Biochem. Biophys. Res. Commun. 161*, 64–68.
Warren, M. S., Brown, K. A., Farnum, M. F., Howell, E. E., & Kraut, J. (1991) *Biochemistry 30*, 11092–11103.
Wells, J. A. (1990) *Biochemistry 29*, 8509–8517.
Wertman, K. F., Little, J. W., & Mount, D. W. (1984) *Proc. Natl. Acad. Sci. U.S.A. 81*, 3801–3805.
Woody, R. W. (1985) *Peptides 7*, 15–114.